

Can crack front waves explain the roughness of cracks ?

E. Bouchaud¹, J.P. Bouchaud², D. S. Fisher^{3,4}
S. Ramanathan⁵, J. R. Rice^{5,6}

October 26, 2018

¹ Service de Physique et de Chimie des Interfaces, Centre d'Études de Saclay, 91191 Gif-sur-Yvette Cedex, France

² Service de Physique de l'État Condensé, Centre d'Études de Saclay, Orme des Merisiers, 91191 Gif-sur-Yvette Cedex, France

³ Physics Department, Lyman Laboratory, Harvard University, Cambridge, MA 02138, USA

⁴ Division of Engineering and Applied Science, Harvard University, Cambridge, MA 02138, USA

⁵ Bell Laboratories, Lucent Technologies, Murray Hill, NJ 07974

⁶ Department of Earth and Planetary Sciences, Harvard University, Cambridge, MA 02138, USA

Abstract

We review recent theoretical progress on the dynamics of brittle crack fronts and its relationship to the roughness of fracture surfaces. We discuss the possibility that the intermediate scale roughness of cracks, which is characterized by a roughness exponent approximately equal to 0.5, could be caused by the generation, during local instabilities by depinning, of diffusively broadened corrugation waves, which have recently been observed to propagate elastically along moving crack fronts. We find that the theory agrees plausibly with the orders of magnitude observed. Various consequences and limitations, as well as alternative explanations, are discussed. We argue that another mechanism, possibly related to damage cavity coalescence, is needed to account for the observed large scale roughness of cracks that is characterized by a roughness exponent approximately equal to 0.8.

1 Introduction

1.1 Experiments

Fracture surfaces are among the best characterized scale invariant objects in nature [26, 6]: crack profiles have been shown to be self-affine objects, sometimes over five decades in length scale (from $r = 5$ nm to 0.5 mm). The roughness exponent ζ that characterizes the typical deviations δh of the surface as a function of distance along the crack surface r (parallel to the front), as $\delta h \sim r^\zeta$, is found to be around $\zeta \sim 0.8$. A typical crack profile is shown in Fig. 1, as an illustration for a rough, self-affine object.

Quite surprisingly, the value of ζ has been found to be to a large degree *universal* [3, 24, 6], i.e. independent of both the material (glass, metals, ceramics, etc.) and of the fracture mode (fatigue, pure tension, stress corrosion, etc.)¹ More recent experiments, however, have suggested a more complex scenario, with at least two different apparent roughness exponents [5, 12, 11]: for a given (macroscopic) crack velocity V_m , the roughness exponent for small length scales $r < \xi_c(V_m)$ is found to be around $\zeta = 0.5$, whereas for large length scales $r > \xi_c(V_m)$, the previous value $\zeta = 0.8$ is observed. The scale $\xi_c(V_m)$ is a crossover length which appears to diverge for $V_m \rightarrow 0$ but becomes irresolvably small for the large V_m that occur in spontaneous dynamic fracture. In this interpretation, the value $\zeta \sim 0.5$ corresponds to behavior associated with *near threshold* crack growth, while $\zeta \sim 0.8$ corresponds to ‘fast’ cracks, for which the effects of the onset are negligible.

As we shall discuss in some detail, it is important to distinguish at least *three* different roughness exponents [6]: one describing the roughness in the direction perpendicular to the crack propagation, a second the roughness in the direction of the propagation, and a third one (which we call ζ_f) describing the *in-plane* roughness of the crack front *during its propagation* through the material. The exponent characterizing this in-plane roughness, which does not directly affect the fracture surface itself, has been measured by two groups [39, 13, 10], on Plexiglas and on metallic alloys respectively. These experiments were performed on *stationary* crack fronts after some growth: a stable crack growth geometry was used in [39, 13], and the front was observed *in situ* (the sample being transparent); more recent experiments during macroscopically slow growth measured successive crack front positions in 0.2 s time increments [25]. In [10], on the other hand, the fracture was stopped before complete failure of the specimen, and the in-plane front morphology was observed after unloading. In both sets of experiments, the front roughness index ζ_f was found to be in the range 0.5 – 0.65, over at least two decades.

¹More details on the experimental situations will be provided in section 4

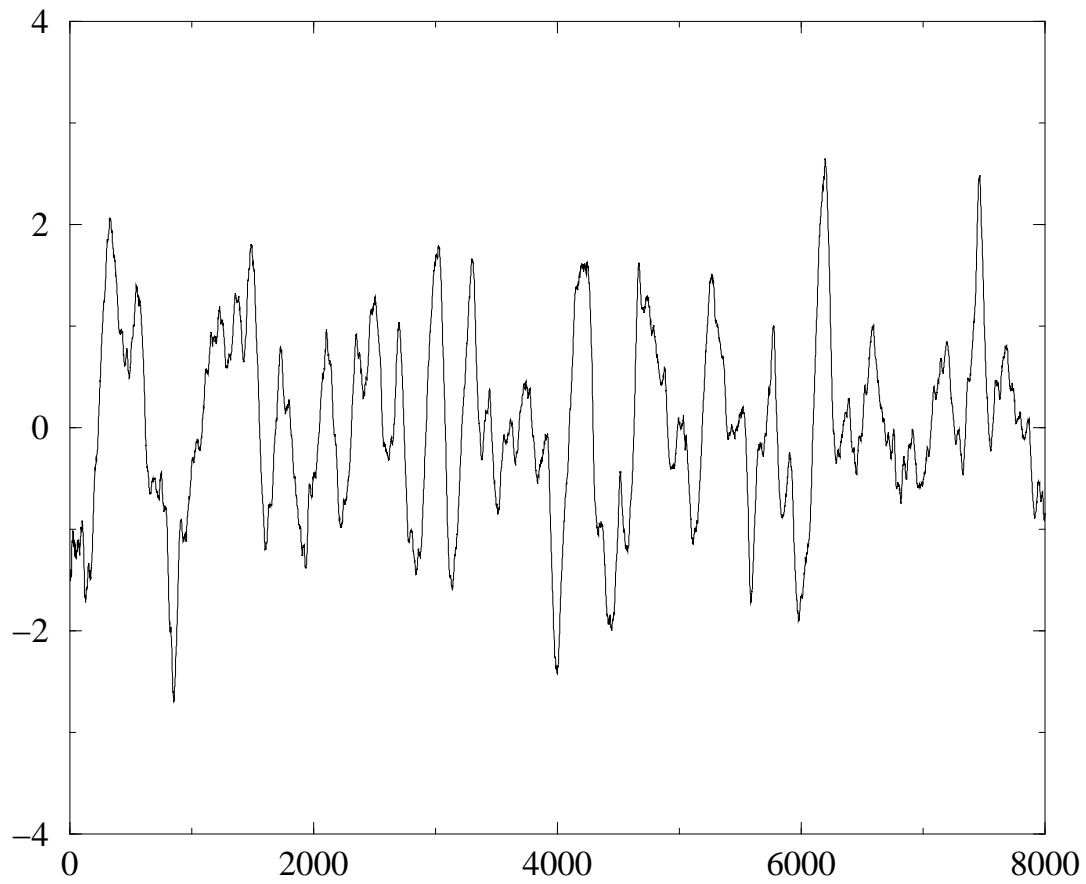


Figure 1: Typical AFM crack profile, measured in a direction perpendicular to the crack propagation. The material in this case is glass broken under stress corrosion. Horizontal and vertical scales are in nanometers. Note that the real slopes are very small.

1.2 Line models

Despite numerous recent efforts, there is unfortunately no satisfactory theory that explains the values of *any* of these exponents. A *qualitatively* useful framework was proposed in [4], in which the crack front was modeled as an overdamped elastic string moving in a random ‘pinning’ environment representing the disordered micro-structure of the material. This picture provides a natural interpretation for the existence of roughness exponents, and also for the appearance of a velocity dependent crossover length separating two regimes: a “critical” or “onset” regime, appropriate to a crack front just barely able to propagate through the material, and an “unpinned” regime, where the front sweeps through the random pinning at a substantial velocity. But this simple elastic-string model is certainly not applicable *quantitatively*.

Refined versions of the crack front model take into account the non-local nature of the elasticity [37, 16, 38, 40]. Long-ranged elastic effects make the crack front much stiffer thereby reducing its roughness (and concomitantly that of the fracture surface). If elastic waves are ignored, this stiffness, combined with the assumption of only short distance correlations in the heterogeneities of the material properties, results in a predicted large scale roughness of both the in-plane crack front and the fracture surface that grows only *logarithmically* with length scale (i.e. $\zeta = 0$) [23, 33]. Although some experiments do indeed observe such weak logarithmic roughness [23], most fracture surfaces appear to be far rougher, at least up to a material dependent length scale, beyond which the roughness saturates (or grows much more slowly [6]).

1.3 Crack front waves

But some important physics was left out of these quasi-static calculations: the effects of dynamic stress transfer along the crack front caused by elastic waves. These were first studied for *cracks restricted to a plane*, numerically by Morrissey and Rice [27] and analytically by Ramanathan and Fisher [32]. It was found that in an ideal material, planar distortions of the crack front could propagate as waves *along* the crack front. Such waves would be generated continuously by local variations in the material properties, particularly in the critical fracture energy, as the crack advances through a disordered material. These waves, established in the framework of the full three-dimensional vectorial elastodynamics [45] suggested that a crack front in an ideal material is even more unstable than had been suggested in the first 3D investigations of dynamic cracking through disordered solids by [31] based on a scalar approximation to elastodynamics. However, these planar waves only directly affect the in-plane roughness of crack fronts rather than the (out of plane) shape of fracture surfaces and, in fact, are predicted to be strongly damped whenever the fracture energy is substantially velocity dependent [32].

Interestingly, another type of crack front wave that *can* radically change the roughness of fracture surfaces was recently discovered by Ramanathan and Fisher [35]. Crack fronts can indeed also support waves that involve *non-planar* deformations of the front, which we will call *corrugation waves* (see also [46] for the perturbative elastodynamic solution for a non planar crack). Although it is not clear at this point whether these waves can propagate forever in an ideally elastic material, they can certainly propagate over long enough distances to have dramatic effects. Recent observations have indeed shown [42] that in glass, perturbations do indeed propagate over long distances. These corrugation waves will be reflected in the fracture surfaces. Indeed, they are probably the explanation of Wallner lines [44, 21], the oft-observed grooves on the fracture surfaces of materials that are broken dynamically.

1.4 Aim of this paper

In this paper, we investigate the effects of these waves on the roughness of fracture surfaces, in particular whether they might provide a natural interpretation for the value of the intermediate length-scale roughness exponent of $\zeta \sim 0.5$. An analogous effect for the in-plane roughness of the crack front was suggested by Ramanathan and Fisher [33] but it was not discussed in detail. Here we will derive the related result for non-planar crack front deformations, and consider both this, and the in-plane case, in a broader context. We will then discuss whether this scenario is compatible with experimental results and make some predictions about its consequences if it indeed is. It is important to stress that the concept of crack waves only makes sense if the crack is moving sufficiently fast, at least instantaneously. This might be the case during localized depinning events (see the recent discussion in [25]), but is perhaps never justified in the case of highly ductile, plastic materials where a $\zeta \sim 0.5$ regime is nevertheless observed. We discuss in the conclusion alternative models that could explain this value of ζ in the absence of crack front waves. Finally, we will discuss a different mechanism that may be involved in the large length scale, $\zeta \sim 0.8$ regime.

2 Crack front dynamics

2.1 Basic ingredients and notations

Let us describe the evolution of the shape of the crack front at time t by two functions, $f(x, t)$ for its position in the plane of the crack (f is for ‘front’) and $h(x, t)$ for its out of plane deformation (h is for ‘height’) with x denoting the coordinate in a direction *parallel* to the crack front. In the following, we choose the y axis in the out-of-plane direction and the z axis in the direction of the crack propagation. (Note that these notations differ from those used in, e.g. [27],

where the coordinate along the crack front is called z .)

In an ideal material with no heterogeneities, the front would be straight and would propagate in a plane at a uniform velocity V (at least below the Yoffe speed) which is a function of the stress intensity factor; i.e., $f(x, t) \equiv Vt$ and $h(x, t) = \text{constant}$. But in a heterogeneous medium, the instantaneous local velocity of the crack front, $V(x, t)$ is constant neither in space nor in time, and is *a priori* very different from the *global macroscopic velocity* V_m , because close to the threshold for crack growth, the crack front progresses in a very jerky, intermittent manner [34].

We will assume a local variation of the material toughness, and therefore of the fracture energy (the critical energy release rate). These heterogeneities affect the dynamics of the crack front in two rather different ways:

- The variations of the local fracture energy result in a perturbation in the local velocity. The resulting change in the shape of the front will modify the stress intensity factor [28, 45] and energy available for fracture at other parts of the crack front thereby affecting the crack velocity at these other points.
- The *direction* of propagation of the crack front can be also affected by local heterogeneities. Although the details of how this occurs locally will depend on the physics in the process zone near the crack front, this should be expected on general grounds: heterogeneities in material properties can change the *local* loading from being purely tensile (as imposed macroscopically) to having a shear component that will tend to make the crack bend in a direction that decreases or even cancels the Mode II component of the local stress intensity [9, 20]. On a more microscopic level, the crack may change direction to go around a tougher region that is located asymmetrically with respect to the local plane of the crack. Any asymmetric local distortion of the crack front which results from these types of heterogeneities will again modify the stress intensity at other points on the crack front, in particular by introducing Mode II (and possibly Mode III) components, thereby causing non-planar deformations of other parts of the crack front as well.

2.2 The physical origin of crack waves

Because stresses are transferred through the medium and along the crack surface by elastic waves – dilatational, shear and Rayleigh – the changes in stress intensity factors caused by a local disturbance will propagate away from their source at velocities of order the sound speed, but the details of this propagation are complicated.

2.2.1 In plane waves

It is instructive to consider what happens to the stress intensity factor along a straight front of a planar crack if one small part of it slows down momentarily for some reason, such as an encounter with a locally tougher region. The initial changes in the stress at other points along the crack front will arrive with the dilatational waves. Perhaps surprisingly, the effects of these will be to *increase* the stress intensity factor thereby tending to make the other parts of the crack *accelerate* rather than decelerate. Only after the Rayleigh waves arrive some time later will the stress intensity factor decrease, soon becoming less than that before the disturbance arrived and hence tending to slow the crack down as one would have expected. The crack front waves are a result of the competition between these two effects: a locally tougher region will initially cause other parts of the crack to accelerate and then cause them to decelerate. In the absence of dissipation, this gives rise to the existence of waves of slowing down and speeding up which can propagate in a self-sustaining manner along the crack front at a speed, c_f (relative to their source), which is slightly less than the Rayleigh wave speed, c_R . These carry distortions of the in-plane crack front position $f(x, t)$.

2.2.2 Corrugation waves

The out-of-plane corrugation waves have a similar origin. A local distortion of the crack front, say in the positive h direction – ‘up’ –, would be expected to result in some Mode II loading at other points on the crack front with a sign which tends to make the crack also bend up at these other points thereby keeping the crack front as straight as possible; indeed, this is just what the static stress changes due to such a distortion will tend to do. But the initial stress changes which arrive with the dilatational waves will have the opposite effect: they carry Mode II stress intensity which tends to make the crack bend *down*. As was the case for the in-plane velocity changes, this bending effect is negated by the Rayleigh waves and at later times the crack will bend in the naively expected ‘up’ direction. The competition between these effects of two types of elastic waves, combined with the tendency of the crack front to bend so as to cancel the Mode II loading, give rise to propagating waves along the crack front and concomitant corrugations in the fracture surface. These waves move with a speed, c_h , which is again slightly slower than c_R and depends weakly on the overall velocity of the crack front.

2.3 An equation of motion for the crack front

Since we are primarily interested in the fracture surfaces, we will focus on the corrugation waves and their effects, returning in section 5.4 to a brief discussion of the in-plane crack front waves.

A small out-of-plane component of the crack front, $h(x', t')$, will give rise to

a Mode II stress intensity factor given by [46]:

$$K_{II}(x, t) = K_I^0 \int_{-\infty}^{\infty} dx' \int_{-\infty}^t dt' h(x', t') Q(x - x', t - t'; V) \quad (1)$$

where the kernel Q is a homogeneous function of $x - x'$ and $t - t'$ of degree -3 which depends on the overall unperturbed velocity of the crack, V ; and K_I^0 is the unperturbed stress intensity factor which we take to be purely Mode I.

We assume that in response to this Mode II local load, the crack will tend to bend so as to decrease the Mode II component of the stress intensity factor. But, as discussed above, the crack front will also tend to bend in response to a local assymetry that we parameterize by a random field $\eta(\mathbf{r})$. A natural assumption with some experimental support is that the crack adjusts in such a way that the net Mode II stress intensity factor is zero [9, 20]:

$$K_{II}(x, t) - K_I^0 \eta(\mathbf{r}) = 0, \quad (2)$$

where η is computed at the current position of the crack front: $\mathbf{r} = (x, y = h(x, t), z = f(x, t))$. Therefore, one has, using Eq. (1):

$$Q \otimes h = \eta \quad (3)$$

everywhere on the crack front and at all times. (Here \otimes is the convolution in x and t that we wrote explicitly in Eq.(1)).

We can invert this to find the response of the crack to a local bending heterogeneity:

$$h = P \otimes \eta \quad P \equiv Q^{-1} \quad (4)$$

The ‘propagator’ $P(x - x', t - t')$ is a complicated homogeneous function of degree -1 which is only known explicitly as an integral expression; it includes the effects of all of the three types of elastic waves.

The above equation (2) assumes that the crack front ‘follows’ perfectly the local randomness. It might be interesting to generalize this equation to describe the fact that the crack will ‘react’ to a change of stress intensity factor with a certain lag. Thus we propose an effective equation of motion for the direction of the crack front of the following form [33, 35] :

$$\frac{\partial^2 h(x, t)}{\partial t^2} = \frac{V^2}{\ell_r} \left(-\frac{K_{II}(x, t)}{K_I^0} + \eta(\mathbf{r}) \right) \quad (5)$$

where ℓ_r is a microscopic ‘adaptation’ length. Intuitively, Eq. (5) means that the local orientation angle of the surface, equal to $\partial h / \partial z$ changes at a rate proportional to K_{II} / τ_r , with $\tau_r = \ell_r / V$. Since the crack is moving at a velocity V , derivatives with respect to z are, for a weakly perturbed crack front, simply related to time derivatives through $\partial z = V \partial t$. On length scales large compared to ℓ_r , one can set the left hand side of equation (5) to zero, and recover (2). In the following, we will assume that the length ℓ_r is microscopic.

2.4 The corrugation waves: diffusion and dispersion

The corrugation waves of the crack front arise from a zero in the Fourier transform of Q at a real (or almost real, see below) value of $\omega/|q| = s_h$ which gives rise to a divergence of P for $(x - x') = \pm s_h(t - t')$ where

$$s_h = \sqrt{c_h^2 - V^2} \quad (6)$$

is the speed of the corrugation waves in the direction parallel to the moving crack front (Note that the total speed c_h relative to the source is indeed given by $c_h^2 = s_h^2 + V^2$).

The wave speed c_h is found to depend weakly on the crack front velocity V : it varies from $0.96 c_R$ when $V \ll c_R$ to c_R as $V \rightarrow c_R$. The numerical solution suggests that c_h has a very small but non zero imaginary part $\epsilon(V)c_R$, with ϵ of order 10^{-4} for small V to $2 \cdot 10^{-3}$ for $V = 0.6c_R$ [35]. This means that, strictly speaking, corrugation waves will not propagate indefinitely. Since ϵ is so small, it is a reasonable approximation to ignore, at least for now, its effects.

The behavior near to this singularity of P , dominates the long time behavior of the crack front. The important parts have the form:

$$P(x, t) \propto \left(\frac{C_b c_s}{x - s_h t} - \frac{C_b c_s}{x + s_h t} \right) \quad (7)$$

(in contrast to a sum of delta-functions at $x \pm s_h t$ for conventional waves). Here C_b is a velocity dependent dimensionless numerical coefficient, and c_s is the shear wave speed. [Note that the dimension of P is $[T]^{-1}$, as it should be since η is dimensionless in Eq. (4), and convolution brings an extra $[L][T]$ factor.] The primary effects of a perturbation propagate away from its source in two directions that are at an angle $\arccos(V/c_h)$ from the direction of propagation of the crack – i.e., almost *parallel* to the crack front for a slowly advancing crack.

From Eq.(7), the shape of any disturbance would persist without broadening for arbitrarily long times (for $\epsilon = 0$). But this result holds only for a perfect elastic medium with an infinitely sharp crack and no lag in response to bending forces (i.e., $\lambda_r = 0$). In reality, the two sharp peaks of Eq. (7) will be broadened by various mechanisms. The first one, discussed by Ramanathan and Fisher [32], is the existence of Kelvin-like viscoelastic effects, i.e. a delay time τ_d between stresses and strains.² This will lead to a diffusive-like spreading of the peaks, with a diffusion constant of the order of $D_d \sim c^2 \tau_d$, whose actual value will involve many details of the relaxation processes as embodied in the frequency

²This effect was not treated correctly in reference [32] due to the nature of the boundary conditions in the moving frame of the crack front. For the case of in-plane cracks discussed there, a detailed calculation has been carried out [14] and leads to qualitatively similar results. In principle, this could also be done for the out-of-plane dynamics although the technical details are likely to be exceedingly cumbersome.

dependence of the elastic moduli [14]. (In the above formula and in the rest of this paper, c denotes a typical wave propagation speed – as far as orders of magnitude are concerned, we do not need to distinguish between the different wave speeds.)

Two other effects are caused by the heterogeneities in the medium in which the elastic waves and the crack front propagate. These inhomogeneities can scatter the (bulk or Rayleigh) elastic waves which mediate the crack front dynamics and thereby give rise to broadening of the ideal crack front waves. But in addition, the small scale corrugations in the fracture surface, created by the heterogeneities and propagated by the crack front waves themselves can act as disorder to scatter the longer wavelength crack front waves. (This may lead to interesting non-linear feedback effects, see [42]). The simplest expectation is that both of these will induce diffusive like spreading of the peaks of Eq. (7) (see e.g. [8]). If the scattering were strong, one would expect the corresponding diffusion constant to be of order $D_s = c\ell_s$, where ℓ_s is the correlation length of the relevant inhomogeneities.

These effects together give rise to a change of the important singular parts of the Fourier transform of the propagator from the ideal case corresponding to Eq.(7) which in Fourier space is:

$$\hat{P}(q, \omega) \sim \frac{C_b c_s}{\omega - s_h |q|} + \frac{C_b c_s}{-\omega - s_h |q|} \quad (8)$$

to

$$\hat{P}(q, \omega) \sim \frac{C_b c_s}{\omega - s_h |q| + iDq^2} + \frac{C_b c_s}{-\omega - s_h |q| - iDq^2}. \quad (9)$$

where $D = D_s + D_d$. The shift of the pole by iDq^2 indeed corresponds to a diffusive damping term of the form $\exp[-Dq^2(t - t')]$ in the time domain.

Physics within the process zone will also affect the propagation of disturbances along the crack front. One might expect that the non-instantaneous response (i.e. $\ell_r \neq 0$) of the crack growth direction embodied in the equation of motion, Eq. (5), would give rise to similar diffusive-like broadening. But in fact, this primarily gives rise to *dispersion* of the waves; this term in Eq. (5) yields, in Fourier space, $-\ell_r/V^2 \omega^2 \hat{h}(q, \omega)$. Since this contribution must be added to Q , one finds that near the poles (i.e. when Q is small), the propagator \hat{P} can be written as:

$$\hat{P}(q, \omega) \sim \frac{C_b c_s}{\omega - s_h |q| - Jq^2 + iDq^2} + \frac{C_b c_s}{-\omega - s_h |q| - Jq^2 - iDq^2}, \quad (10)$$

which is valid when both q and one of $\omega \pm s_h |q|$ are small. Here, the coefficient J that describes dispersion effects is given by $J = C_b c_s s_h^2 \ell_r / V^2$. As will be clear below, however, dispersion effects will not drastically affect the roughness statistics.

Fourier transforming Eq. (10) gives rise to the final form of the propagator, which is a sum of a right moving contribution $P^R(x, t)$ that depends on $\chi_R = x -$

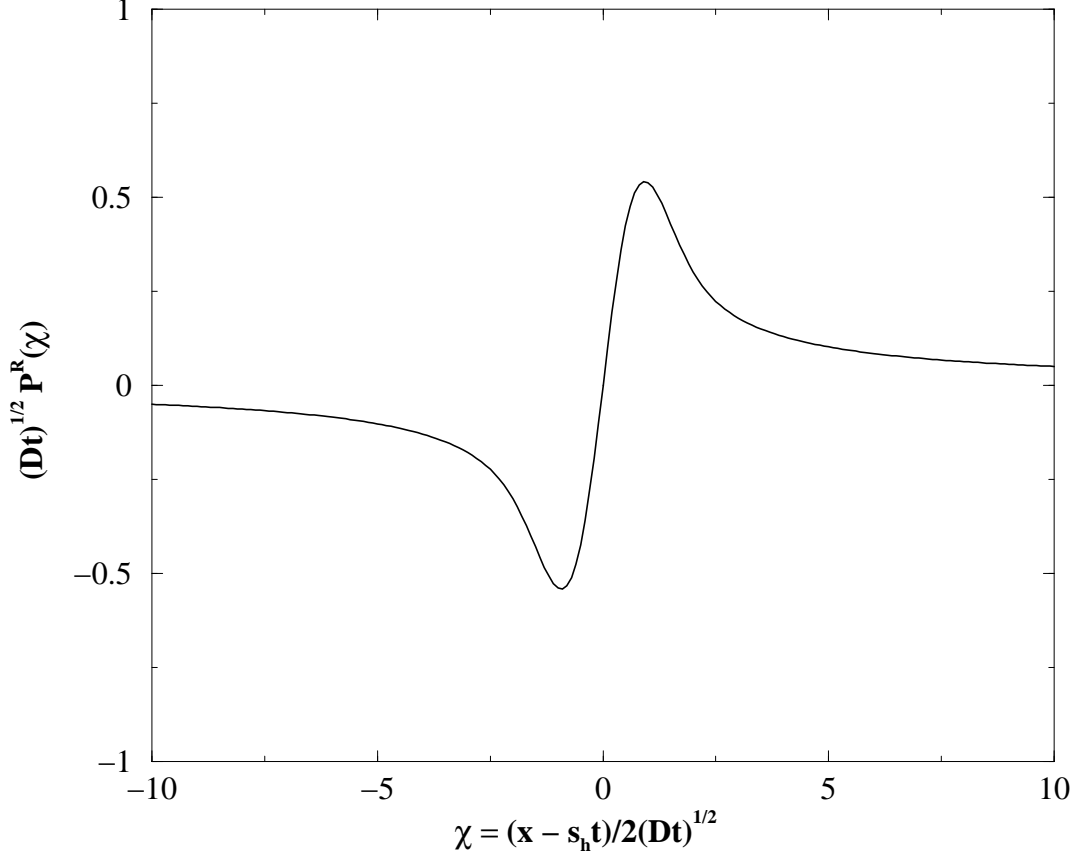


Figure 2: Shape of the rescaled propagator $P(\tilde{\chi})$ as a function of the rescaled variable $\tilde{\chi} = (x \pm s_h t)/2\sqrt{Dt}$. Here we have set $C_b c_s/2\sqrt{\pi} = 1$.

$s_h t$ and a similar left moving contribution $P^L(x, t)$ that depends on $\chi_L = x + s_h t$. We find:

$$\begin{aligned}
 P^R(\chi_R) &\approx C_b c_s \int_0^\infty \frac{dq}{\pi} \sin(q\chi_R + Jq^2 t) e^{-Dq^2 t} \\
 &\approx \frac{C_b c_s}{2\sqrt{\pi Dt}} \Im \left[\exp(-\tilde{\chi}_R^2) \operatorname{erfc}(-i\tilde{\chi}_R) \right], \quad \text{with} \quad \tilde{\chi}_R \equiv \frac{\chi_R}{2\sqrt{(D + iJ)t}}.
 \end{aligned} \tag{11}$$

In the above equation, erfc is the complementary error function, and \Im denotes the imaginary part. The above result holds for $|\chi_R| \ll s_h t$ since we have used the expression of the propagator Eq. (10) which is only valid close to the pole.

For $J \ll D$, (12) is an antisymmetric function of χ_R which decays as $1/\chi_R$ for $\chi_R \gg \sqrt{Dt}$ (in agreement with Eq. (7) above), vanishes linearly for $\chi_R \ll \sqrt{Dt}$, and has a peak (trough) for $\chi \sim \pm\sqrt{Dt}$. This function is plotted in Fig. 2. Interestingly, this shape is similar to what has been observed in [42].

3 Corrugation wave mediated roughening

3.1 Quantities of interest

The dependence of the random local bending tendency, η (see Eq. (5)), on h does not play an important role, and we assume a simple form for its random dependence on x (the direction along the crack front) and z (the direction parallel to crack propagation): Gaussian with mean zero and covariance given by

$$\langle \eta(x, z) \eta(x', z') \rangle = \sigma^2 \mathcal{G} \left(\frac{(x - x')^2 + (z - z')^2}{\xi_0^2} \right) \quad (12)$$

with σ , the dimensionless root mean square amplitude of the random bending, \mathcal{G} a certain short range function and ξ_0 the correlation length of this randomness. In a disordered material, there are a priori many different length scales associated to different types of heterogeneities: size of precipitates, microcavities, metallurgical grains, quenched in stresses, etc. The relevant heterogeneities will actually depend on the observation scale. In the following, for simplicity, we will assume that we are only interested in length scales large compared to ξ_0 , and replace the function \mathcal{G} by a (two dimensional) δ -function. This might however not always be justified (see section 5.4 and [40]).

The existence of crack front waves means that a local variation of the material properties that is anisotropic or located just off the plane of the crack, say near $(x_0, z_0) = (x_0, Vt_0)$, will result in a perturbation $h(x, t)$ of the deviation of the crack from planar which propagates, relative to (x_0, z_0) , at a velocity c_h . Using the results of the previous section, the perturbation induced by a variation $\eta(x_0, z_0)$ can be written as [27, 28]:

$$h(x, t) = \int_{-\infty}^{+\infty} dx_0 \int_0^t dt_0 \left[P^R + P^L \right] (x - x_0, t - t_0) \eta(x_0, z_0 = Vt_0), \quad (13)$$

where $t = 0$ is the time at which the front penetrates into the disordered region. Again, we have assumed that the perturbation from a straight front is small in order to replace z_0 by Vt_0 .

From this expression, one can compute the correlation function of the fracture surface heights from the function:

$$B(r_x, r_z) = \left\langle [h(x + r_x, z + r_z) - h(x, z)]^2 \right\rangle, \quad (14)$$

that is often measured experimentally. The brackets refer to an average over the point (x, z) , which — provided the measurements are taken in a region sufficiently far from where the crack front enters the random heterogeneities and starts to roughen, and sufficiently small so that the crack does not accelerate — can be replaced by an average over the randomness. The roughness exponent ζ , is defined by $[B(\mathbf{r})]^{1/2} \sim |\mathbf{r}|^\zeta$, and may in general depend on the direction of \mathbf{r} . The roughness of the fracture surface reflects the temporal history of the non-planar deformations of the crack front.

3.2 Roughness correlation function

It is instructive to consider how a given ‘asperity’ (i.e. a given local variation of the material properties) — located at (x_0, z_0) — contributes to the roughness correlations. The dominant effects of this asperity will be carried by the left and right moving corrugation waves, with a diffusive-like spreading of these waves in time. Points outside of these spreading waves will not be affected appreciably. If the two points of interest \mathbf{r}, \mathbf{r}' are both affected by the waves, the resulting deformations of the crack front at the two points are highly correlated and do not contribute much to $B(\mathbf{r})$ unless:

- either their separation in time, $|r_z/V|$, is comparable or greater than the time, $(z - z_0)/V$, since the waves left the asperity;
- or their separation perpendicular to the direction of propagation, $|r_x - s_h r_z/V|$ for the right-moving waves, is comparable to or greater than the diffusive spreading, $\sqrt{Dr_z/V}$.

Thus the dominant contributions to the mean-square height differences will be from asperities which are *within* a parabola opening backward from one of the points with its axis along the wave direction, but *not within* the similar parabola opening backward along the same wave direction from the other point (see Figure 3).

The mean-square roughness is approximately given by a sum of two terms, one from the right-moving and the other from the left-moving waves. The effects of the cross-terms between the right and left moving waves are small, because they carry signals that come from uncorrelated asperities. We find that:

$$B(\mathbf{r}) \approx \frac{4C_b^2 \sigma^2 \xi_0^2 c_s^2}{V} [\mathcal{F}(|r_x - s_h r_z/V|, r_z) + \mathcal{F}(|r_x + s_h r_z/V|, r_z)] \quad (15)$$

where the function \mathcal{F} has the following asymptotic behaviour:

$$\mathcal{F}(|\chi|, r_z) \approx \frac{|\chi|}{2D} \quad (16)$$

for $|\chi| \gg \sqrt{Dr_z/V}$ and

$$\mathcal{F}(|\chi|, r_z) \approx \sqrt{\frac{r_z}{\pi V D}} \frac{\cos \theta/2}{\cos^2 \theta}, \quad (17)$$

where $\tan \theta = J/D$, for $|\chi| \ll \sqrt{Dr_z/V}$.

Let us comment these results. First consider the roughness measured *perpendicularly* to the direction of crack propagation, i.e. along the x direction, which corresponds to $r_z = 0$. We find that the roughness is given by:

$$\delta h(r_x) \sim \sigma \xi_0 c_s \sqrt{\frac{r_x}{DV}}. \quad (18)$$

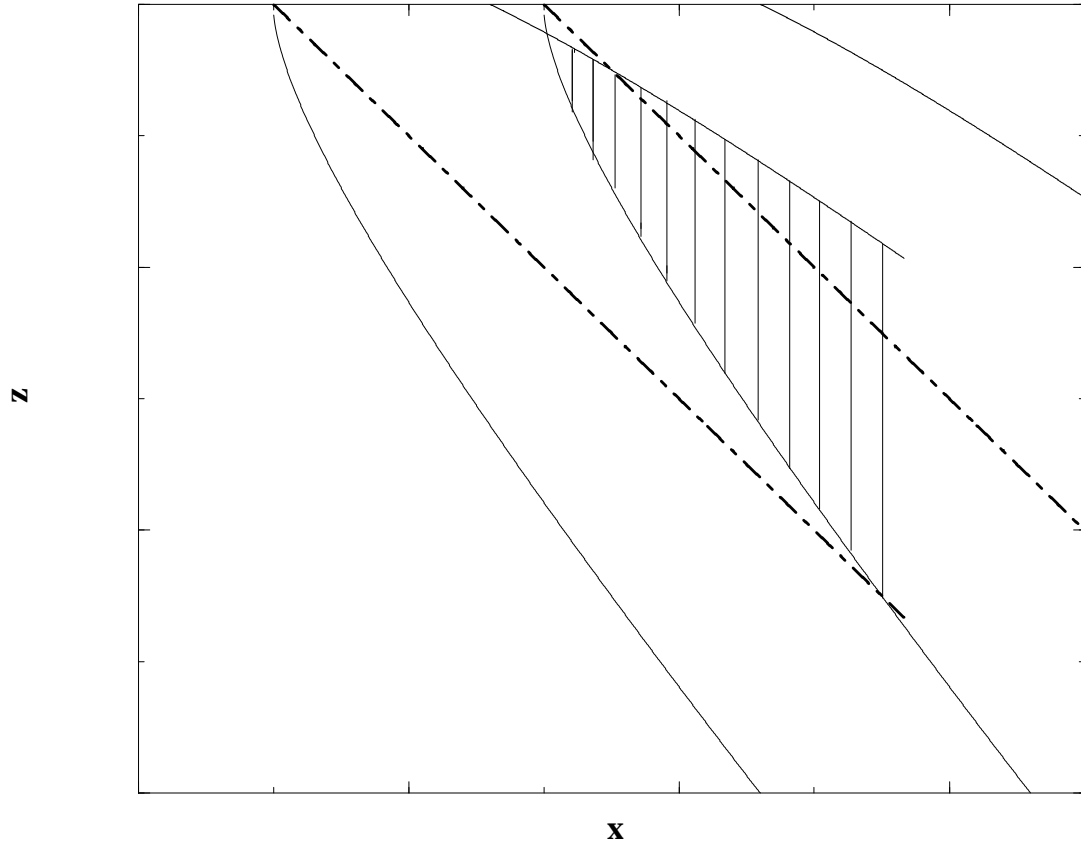


Figure 3: The contribution to the difference of roughness between two given points comes from asperities within parabolas opening backwards along the wave propagation direction, but not from their common intersection (hatched region).

Note that if the distance traveled by the crack since it entered the disordered region is finite and equal to $L(=Vt)$, the above result is only valid if $r_x \ll \xi_L$, with $\xi_L = \sqrt{DL/V}$. For longer distances, the roughness saturates in this regime.

In the direction *parallel* to the crack propagation — i.e. perpendicular to the crack front, $r_x = 0$ — the roughness is given by

$$\delta h(r_z) \sim \sqrt{\frac{s_h}{V}} \sigma \xi_0 c_s \sqrt{\frac{r_z}{DV}}, \quad (19)$$

i.e the roughness is reduced by a factor of order $\sim \sqrt{c/V}$ compared to that in the x direction. This difference in the amplitudes in the two directions should be very pronounced at low crack growth velocities.

Another notable effect of roughness due to corrugation waves is that along the direction of propagation of the crack front waves, i.e. for $r_x = s_h r_z / V$, one expects to observe ridges and grooves oriented in these directions. The long-distance roughness is somewhat suppressed in the wave directions where one finds:

$$\delta h \sim \sigma \xi_0 c_s \left(\frac{r_z}{V^3 D} \right)^{1/4}, \quad (20)$$

which is a factor $(VD/c^2 r_z)^{1/4}$ smaller than in the direction parallel to the crack propagation, where it is already reduced compared to that in the x direction. Interestingly, if such a reduced roughness direction is observed it could be used to *determine* the local velocity V at which the crack was propagating [42].

Note that the above results for the roughness exponents obtained here ($\zeta = 1/2$ or $1/4$ in a particular direction) are, largely coincidentally, identical to that for an over-damped elastic line driven through random impurities (the so called Edwards-Wilkinson model [1]). This is in spite of the fact that the elasticity of a crack front is non local (i.e., it is described by a $|q|$ wave-vector dependence of the energy, rather than the q^2 dependence of the oversimplified string model). This non local elasticity is in a sense responsible for the existence of crack waves; however, the diffusive spreading of these waves is eventually the dominant factor that determines the statistics of the crack roughness; this is the cause for the equivalence of the roughness exponents to that of the elastic string with diffusive dynamics.

So far, we have ignored the effects of the small imaginary part $\epsilon(V)c_R$ of the corrugation wave velocity. At sufficiently long times, this will damp the waves more rapidly than diffusively. The decay of the effects of a localized perturbation will eventually change from the $1/\sqrt{Dt}$ decay of the peaks in h (see Eq. (10)) to $1/\epsilon(V)ct$ at longer times. But the crossover time will be of order $t_\epsilon \sim D/\epsilon^2 c^2$. In directions parallel to the crack front the roughness will thus only be reduced on length scales larger than $\xi_\epsilon \sim D/\epsilon c^2$ which is macroscopic even if D/c is nanometric. Perpendicular to the crack front, the reduction of the roughness will occur on scales smaller by a factor V/c . On asymptotically long length scales,

the predicted roughness would be reduced to its logarithmic form found in the absence of crack front waves but with an amplitude increased by a factor $1/\epsilon(V)$.

4 Comparison with experiments

In this section, we will compare the above predictions with several experimental observations on materials as different as glass, intermetallic-based or metallic-based alloys, fractured in stress corrosion, fatigue or pure tension. Our main prediction (Eq. (18)) concerns the amplitude and form of the roughness correlations in the regime in which crack wave dynamics dominate. In two of the experiments described below, it was found that in the regime where $\zeta \sim 0.5$, the roughness amplitude is approximately independent of the *macroscopic average* crack velocity V_m [12]. Only the crossover scale ξ_c , which is the upper limit of this regime, is found to depend on V_m . This suggests that the *local* crack velocity V that enters Eq. (18) may actually be roughly constant during localized de-pinning events and we will assume V to be a significant fraction of the Rayleigh velocity c_R .

Assuming that the viscoelastic broadening is the dominant effect (compared to the scattering of the crack waves), one can write $D \sim c^2 \tau_d$, such that Eq. (18) finally reads (for $V \sim c$):

$$\delta h \sim \xi_0 \sqrt{\frac{r_x}{c \tau_d}}, \quad (21)$$

assuming strongly disordered materials, for which $\sigma = O(1)$. It is reasonable to estimate the value of τ_d (which measures the viscoelastic lag between stresses and strains) as a typical vibrational time $\tau_d \sim a/c$ where a is an atomic distance. This leads to $\tau_d \sim 10^{-12}$ seconds.

4.1 Stress corrosion of glass

Four point bending experiments on soda-lime silica glass leading to stress corrosion fracture were performed in a controlled humidity environment. Typical values of the macroscopic average crack velocity V_m are $V_m \sim 10^{-9} - 10^{-5}$ m/s. The regime where $\zeta = 0.5$ is found to extend between 1nm and tens of nanometers for the lowest velocities V_m . It is reasonable to assume that in this material ξ_0 is of the order of the size of three to six silica tetrahedra, i.e $\xi_0 \sim 1$ nm, corresponding to the smallest scale of density fluctuations [43]. Taking $c \sim 2 \cdot 10^3$ m/s and $\tau_d \sim 10^{-12}$ seconds, Eq. (18) leads to $\delta h \sim 2$ nm for $r_x = 10$ nm, which corresponds well to observations in atomic force microscopy (AFM), (see [12] and Figure 1).

The corresponding value of the crossover length ξ_L above which the effects of the macroscopic geometry dominate, is larger than $10\mu\text{m}$ for a typical sample size of $L = 1$ cm. Since this is much larger than the crossover scale $\xi_c(V_m)$ separating

the $\zeta = 0.5$ from the $\zeta = 0.8$ regime in this material, the finite sample size effects should not matter.

4.2 Fatigue of a Ti₃Al-based alloy

Fatigue experiments were carried out on compact tension specimens of a Ti₃Al-based alloy at a frequency of 30 Hz with a constant R-ratio of 0.1. Varying the maximum load allowed us to vary the average crack velocity again between $V_m = 10^{-9}$ and 10^{-5} m/s.

This alloy contains faggots of needle shaped precipitates (of size $20/1\mu\text{m}$) of the brittle α_2 phase in the more ductile β phase. The fracture mode was observed *in situ* using scanning electron microscopy (SEM). Cleavage cracks open in the α_2 precipitates, blunt when extending into the β matrix and finally coalesce together and with the main cracks.

The $\zeta = 0.5$ regime is in this case observed at least down to $r \sim 10^{-2}\mu\text{m}$ and up to $\xi_c = 10\mu\text{m}$ for the lowest velocities V_m . It is reasonable to think that ξ_0 corresponds to the size of heterogeneities contained within a needle, and hence significantly smaller than $1\mu\text{m}$. Taking for ξ_0 the lower limit of the scaling region $10^{-2}\mu\text{m}$, one finds (with $c = 5 \cdot 10^3$ m/s and $\tau_d = 10^{-12}$) $\delta h \sim 0.5\mu\text{m}$ for $r_x \sim 10\mu\text{m}$, which again concurs with experimental findings [12] for which both AFM and SEM were used. Similar orders of magnitude are found in the case of pure tension fracture for which V_m is expected to be much larger [11].

The scale ξ_L is again found to be tens of microns for $L = 1$ cm, which is only of the same order of magnitude as the observed crossover scale $\xi_c(V_m)$ for the smallest V_m studied in [12].

4.3 Fracture of ductile aluminium alloys

Compact tension specimens of a ductile commercial aluminium alloy, 7010, were broken in fatigue at a frequency of 10 Hz and a constant R ratio 0.1. Measured average crack velocities V_m were ranging between $2 \cdot 10^{-9}$ m/s to 10^{-5} m/s. The largest value of the crossover length $\xi_c(V_m)$ did not exceed $0.1\mu\text{m}$ in this case. Note that the values of $\xi_c(V_m)$ are in this case always much smaller than the plastic zone size.

Taking again for ξ_0 the lower limit of the scaling region, i.e. $0.01\mu\text{m}$ and still $\tau_d \sim 10^{-12}$ s, one finds $\delta h \sim 0.02\mu\text{m}$ for $r_x \sim 0.1\mu\text{m}$ whereas SEM observations [7] lead to $\delta h \sim 0.06\mu\text{m}$ for the same r_x . The agreement is in this case more surprising since in this alloy the growth of damage cavities should be dominated by plastic flow rather than crack front motion and hence a longer τ_d might be more reasonable. However, a recent direct study of these cavities using AFM [30] has revealed a clearly anisotropic morphology, where roughness amplitudes, in the direction where the exponent 0.5 is observed, are indeed similar to the ones measured at small length scales on fracture surfaces. Furthermore, the

predicted orders of magnitude are also compatible with the results found on a rapidly quenched aluminium alloy of a different composition, in which the local porosity resulting from the elaboration process might play an important role in the nucleation of damage cavities.

It would obviously be interesting to obtain more direct estimates of D (or equivalently τ_d) and ξ_0 to check whether the above order of magnitudes in the different materials are consistent. However, overall, the scenario in which the small length scale exponent of 0.5 is due to the existence of diffusively broadened crack front waves in localized depinning events appears to be reasonable, at least in the more fragile samples.

5 Physical discussion

We have found that a model of diffusively damped crack front waves naturally leads to a steady state roughening of fracture surfaces induced by the presence of random local heterogeneities, with a roughness exponent $\zeta = 0.5$, that could be the explanation for part of the experimental data. However, there are many limitations to this result and complications that we expect on theoretical grounds. These we now discuss.

5.1 The low velocity limit

As is apparent from the linearized analysis discussed in this paper, the effects of the randomness become larger and larger at low velocities: see Eq. (18). In addition, as shown by Eq. (19), lower velocities give rise to more and more anisotropy. Thus at some velocity, the linearized analysis will almost certainly breakdown. It is just such an apparent divergence in a linearized analysis that signals entry into the “critical” regime in which the motion of the crack front changes qualitatively and becomes intermittent. The non-linearities inherent in the dependence of the heterogeneities on the crack front position through the random function $\eta[x, Vt + f(x, t)]$ in Eq. (5) will then become important.

It is instructive in this context to first consider the case that is best understood theoretically: the *in-plane* deformation of a crack front in the absence of elastic waves [37, 34]. In this case, a moving crack front has only logarithmic roughness at long scales, as mentioned earlier. But at low crack velocities, this result obtains only for length scales longer than a correlation length $\xi(V)$ that diverges as a power of V . On smaller length scales, the physics is quite different, being dominated by the irregular start-stop motion characteristic of the non equilibrium dynamic critical-point at which the crack starts to advance. At the critical point, and for an advancing crack on length scales smaller than $\xi(V)$, the roughness of the crack front is determined by the avalanche-like processes by which the crack starts growing. The important non-linearities in this regime are those in

the random dependence of the local fracture energy on the position of the crack front. These give rise to a critical crack-front roughness exponent predicted to be $\zeta_f \geq 1/3$, *larger* than that in the moving “phase” ($\zeta_f = 0$) [22]. At this point, the effects of elastic waves on the onset of advance of planar cracks in randomly heterogeneous media are not understood, although some indications suggest that the critical behavior may be similar to that in the absence of elastic waves [41].

Similarly, in the case of primary interest to us, non planar crack front deformations, the whole concept of perturbing around a uniformly growing crack front is likely to lose its meaning at low velocities. This is because any given portion of the crack front is likely, as in the absence of crack waves, to spend most of its time essentially stationary, only occasionally advancing in a very jerky manner. This type of irregular local crack growth may well be incompatible with the propagation of corrugation waves. Nevertheless, another type of wave may well play an important role in the onset of crack growth and the roughness fracture surfaces at low [34] velocities. As discussed in [34], there are circumstances in which one might have shock waves of starting or stopping propagating along the crack front. If these involve a substantial non-planar component, then they would certainly affect the fracture surfaces.

A last problem is suggested by geometry: the fact that the angle of propagation of the corrugation waves — if they do in fact still propagate at low crack velocities — will be almost parallel to the crack front. As the crack progresses, they and the sound and Rayleigh waves associated with them will be reflected off the surfaces of the sample further complicating their effects.

Since experiments report a $\zeta = 0.5$ regime for rather small average crack velocities (see section 4), with an amplitude that is, as mentioned above, found to be *independent* of the velocity [12], one could argue that even though the macroscopic velocity V_m is small, the instantaneous velocity during an ‘avalanche’ in a strongly heterogeneous medium is a substantial fraction of the Rayleigh speed so that the present analysis might (at least qualitatively) applicable.

5.2 Non-linearities for rapidly advancing cracks

As noted above, the corrugation wave induced roughness discussed here is similar to that for an over-damped elastic line driven through random impurities. For elastic lines, it is known that certain non-linearities can qualitatively change the behavior, including the roughness exponent [4]. It would thus be interesting to study in the context of fracture surfaces the effects of possible non-linearities. Preliminary indications are that for diffusively broadened crack corrugation waves traveling through a random medium, non-linearities that arise from deformations of the crack are *marginal* in the sense that one needs to go beyond a leading order perturbative analysis in the non-linearities to see whether they will alter the value

of the roughness exponent ζ .³ It is thus plausible that these non-linearities could give rise to the apparently universal exponent for fracture surface roughness. But whether or not this is the case, the marginality suggests that whatever the correct asymptotic behavior, one expects on general grounds that one could observe the linear roughness exponent $\zeta = 1/2$ over a substantial range of length scale before possibly crossing over to a different value, perhaps $\zeta = 0.8$ on longer scales. [The crossover length is expected to be a function of the amplitude of the non-linearity (a priori of order unity but there could be small factors such as $\epsilon(V)$), the strength of the disorder σ , and the front velocity V .] It would be interesting (although a real technical challenge) to work out the theory in detail and to decide whether or not the seductive scenario, where the exponent $\zeta = 0.8$ is produced by the non-linear interaction of corrugation waves, is plausible. As argued below, however, a perhaps more physically likely scenario for this crossover involves damage cavities and their coalescence.

Recent experiments on dynamic fracture of glass by Sharon and Fineberg [42] have observed crack front deformations caused by surface imperfections that propagate for long distances. These involve both small amplitude corrugations – with a shape qualitatively similar to figure 2 — and much larger modulations of the crack velocity and the concomitant in-plane deformation of the crack front. Surprisingly, these pulses seem to propagate without appreciable attenuation and have a shape of the corrugations that is scale independent over more than an order of magnitude in length scale. The authors indicate that these and other features of their experiments suggest that the pulses have a soliton-like character indicative of the importance of non-linearities in spite of the small amplitude of the corrugations. Non-linear effects will in general involve both in-plane and out-of-plane deformations. Via the existence of small dimensionless numbers such as $\epsilon(V)$ and $(c_f - c_h)/c_R$, where c_f is the speed analogous to c_R for in-plane waves [32, 28], these could perhaps give rise to appreciable non-linear effects even with small amplitude corrugations. In any case, the observations provide clear evidence for the existence of crack front waves and suggest that non-linear interactions between them may be important at least in some regimes.

5.3 Long-range correlated heterogeneities

Another effect that could change the roughness exponent of fracture surfaces is long-range correlations in the randomness that we have not considered so far. As discussed in reference [33], correlations in the residual stresses in a material

³Because of the homogeneity of the elastodynamics equations, the non linearities associated with deformations of the crack front will be of order h^3/λ^3 for wavelengths of order of λ . Non linearities of the Kardar-Parisi-Zhang type $(\partial_x h)^2$ or $(\partial_z h)^3$ are known to become marginal in $d = 2$ dimensions [1], whereas the front is a $d = 1$ dimensional object. However, in the presence of diffusively damped linear propagating waves, one can readily show that the ‘lower critical dimension’ where the non linearity is marginal is shifted from $d = 2$ to $d = 1$.

can affect the roughness of fracture surfaces by inducing random Mode II loading on the crack front as the crack grows and relieves the residual stresses. If these frozen-in stresses have correlations that decay as a sufficiently small power law of distance, they will cause the surface to be rougher than it would otherwise have been. Sufficiently long range correlations will cause a positive ζ in the quasi-static case and a $\zeta > 1/2$ in the presence of elastic waves. Whether long-range correlated residual stresses could by themselves cause the observed $\zeta \simeq 0.8$ is not clear, but, if this were indeed the correct cause, one would be left with the problem of understanding why similar power-law stress correlations are so ubiquitous.

5.4 In-plane crack front roughness

It is tempting to attribute the observed crack front in-plane roughness exponent ζ_f of about 0.5 to planar crack-front waves interacting with random impurities in a manner analogous to that analyzed in this paper for the corrugation waves. Evidence for propagation by localized depinning has been obtained for fracture of a weakened interface between plexiglass plates [25], although the average speed of events between the recordings of crack front position, at 0.2 s intervals, is less than about 50 mm/s, and we cannot be sure that the events are actually dynamic in the sense of being inertially controlled. The problem with the dynamic depinning interpretation for in-plane roughening is the effect of velocity dependent fracture energy on the crack front waves. Since the in-plane crack front waves change the local velocity of the front (at variance with the out-of-plane waves), any velocity dependence of the fracture energy will feed back into the dynamics of these waves. As shown in [32], velocity strengthening damps the planar front-waves — essentially by making their velocity complex — while velocity weakening drives the crack front unstable at finite wavelengths. Thus unless the velocity strengthening is, fortuitously, extremely small (as is probably the case for glass [42]), or the crack somehow adjusts its velocity to a point of marginal stability, in a real material planar crack-front waves are unlikely to exist over a wide enough range of length scales to appreciably increase the roughness from the logarithmic behavior predicted for a moving crack with quasi-static dynamics.

Since experiments that have measured crack front roughness have either been on stopped cracks or on — at least apparently — very slowly advancing cracks [10, 39, 13], one would guess that the *critical* crack front roughness discussed in section (5.1) would be what is observed. It is somewhat puzzling, therefore, that the experiments have consistently observed front roughness exponents of order 0.5 – 0.65 rather than $1/3$ (or even $\zeta_f \approx 0.39$, as suggested by a recent numerical simulation [22].) Note that a similar value has been found for the roughness of a slowly advancing contact line [17], a problem that is expected to be in the same universality class as that of crack fronts since the quasi-static, linearized version of the two problems are the same. A possibility, discussed in [40], is

that the correlation length of the heterogeneities is substantial. In the slowly moving regime, this could lead to a short length scale exponent of $\zeta_f = 1/2$ that crosses-over to $\zeta_f = 1/3$ for large distances (see also [19]).

6 From corrugation waves to coalescence of damage cavities ?

As discussed above, the analysis we have done only makes sense when the moving crack front can support corrugation waves. We have already raised some concerns about whether this will be the case at low velocities. But even in high velocity regimes in which these considerations do not play a role, one must certainly require that the very concept of a *single* crack front makes sense. Various observations suggest that, in many materials, this may only be true at small enough length scales as the growth of cracks in many complex materials (possibly including amorphous glassy materials) appears to occur by the nucleation, growth and coalescence of damage cavities in the region surrounding the main crack front (see the discussion in [36]). In such materials, the notion of a well defined moving crack front only makes sense *locally*. One thus might expect that inside a growing cavity one would observe a roughness exponent close to 0.5 [30]. This 0.5 exponent could be due to the mechanism discussed here which would be plausible if the local growth speed of the crack within a cavity were always fast – or of a different origin, as discussed further in the conclusion. But in any case, on length scales larger than the typical size of the cavities when they coalesce, one should observe a crossover to a new regime, dominated by inter-cavity correlations [15]. A natural supposition is that it is the physics of the formation and coalescence of the cavities which is responsible for the observed roughness exponent of $\zeta \simeq 0.8$ for which there is no theory at present. This scenario was proposed in [30], based on the observation of the roughness of growing cavities before coalescence in an aluminum alloy. Qualitatively similar ideas can also be found in [36].

If one assumes that there is a nucleation rate γ per unit time and unit length of new cavities ahead of the crack front, the typical coalescence time of the cavities, t_c , is given by:

$$\gamma \times (V_c t_c) \times t_c \sim 1, \quad (22)$$

where V_c is the speed at which the cavities grow. The above equation means that on the length scale $V_c t_c$ and time scale t_c one cavity will typically encounter another one; $V t_c$ will be the size of the coalescing cavities and thus the crossover length ξ_c . Therefore:

$$\xi_c \sim \sqrt{\frac{V_c}{\gamma}}. \quad (23)$$

Since γ is expected to grow rapidly with the external stress, and therefore with

the macroscopic crack velocity V_m , this scenario could be compatible with the observed *decrease* of ξ_c with increasing V_m .

In summary, we have argued that a crack-wave induced roughness exponent $\zeta = 0.5$ could hold over a range of length scales r , limited above by $r < \xi_c$, the scale of cavity coalescence. For very low macroscopic crack velocities ξ_c may well exceed the maximum lengths observed, while for larger crack velocities, the crossover length ξ_c would decrease into the observable range.

Needless to say, a statistical model based on the idea of cavity coalescence that would reproduce the correct large scale value of $\zeta = 0.8$ is yet to be constructed.

7 Conclusion

In this paper, we have reviewed some recent results concerning crack front waves. We have argued that out-of-plane *corrugation* waves should strongly influence the roughness of fracture surfaces. The diffusive damping of these waves give rise to roughness exponents that are similar to those obtained in the Edwards-Wilkinson model, although the underlying physics is very different. Our central prediction is that the roughness exponent is – assuming short range correlations in the disorder – $\zeta = 1/2$, except along two particular directions (those corresponding to the propagation of the crack front waves) where it is $1/4$. Furthermore, the roughness is predicted to be strongly anisotropic for cracks with instantaneous velocity much smaller than the Rayleigh speed. Although order of magnitudes on existing profiles are compatible with this scenario, a direct experimental examination of these predictions would be very instructive.

We have discussed various limitations and complications that could obscure or even modify these results. We have speculated on the role of damage cavity coalescence, and the corresponding breakdown of the very concept of a single crack *front*, to explain the still mysterious universal value $\zeta = 0.8$ value of the roughness exponent at large length scales.

Finally, we should mention that a value of ζ close to 0.5 for fracture surfaces has also been found for minimal energy surfaces (see the discussion in [18, 2]), quasi-static scalar plasticity (discrete [2] or continuous [33]) models and quasi-static vectorial discrete models [29], where the concept of crack front waves is irrelevant. These models might be more relevant to explain the exponent $\zeta \sim 0.5$ found on fracture surfaces (or cavity surfaces) of highly ductile, plastic materials where the instantaneous velocity is probably always small. The fracture surfaces obtained in these models are expected to be isotropic, at variance with the above prediction based on corrugation waves. This feature should allow to distinguish the two mechanisms.

Acknowledgments: J.P.B. wants to thank Harvard University for hospitality

during the period when this work was completed. Interesting discussions with J. Sethna are gratefully acknowledged. DSF thanks the National Science Foundation for support via DMR-9630064 and DMR-9809334. JRR thanks the Office of Naval Research for support via grant N00014-96-10777.

References

- [1] for an introduction, see A. L. Barabasi, H. E. Stanley, ‘Fractal concepts in Surface Growth’, Cambridge University Press, 1995.
- [2] G. Batrouni, A. Hansen, *Fracture in three-dimensional fuse networks*, Phys. Rev. Lett. **80** (1998) 325
- [3] E. Bouchaud, G. Lapasset, J. Planès, *Fractal dimension of fracture surfaces: a universal value ?*, Europhys. Lett., **13**, (1990), 73.
- [4] J.-P. Bouchaud, E. Bouchaud, G. Lapasset, J. Planès, *Models of fractal cracks*, Phys. Rev. Lett. **71**, (1993) 2240.
- [5] E. Bouchaud, S. Navéos, *From quasi-static to rapid fracture*, J. Phys. I France **5**, (1995) 547;
- [6] For a review, see: E. Bouchaud, *Scaling properties of cracks*, J. Phys. Condensed Matter **9** (1997) 4319
- [7] E. Bouchaud, M. Hinojosa, unpublished.
- [8] see e.g.: P. Claudin, J.P. Bouchaud, M. E. Cates, J. Wittmer, *Models of stress propagation in granular media*, Phys. Rev. E, **57** (1998) 4441
- [9] B. Cottrell, J.R. Rice, *Slightly curved or kinked cracks*, Int. J. Frac. **16** (1980) 155
- [10] P. Daguer, E. Bouchaud, G. Lapasset, *Roughness of a crack front pinned by microstructural obstacles*, Europhys. Lett. **31** (1995) 367.
- [11] P. Daguer, S. Hénaux, E. Bouchaud, F. Creuzet, *Quantitative analysis of a fracture surface by Atomic Force Microscopy*, Phys. Rev. **E53** (1996) 5637.
- [12] P. Daguer, B. Nghiem, E. Bouchaud, F. Creuzet, *Pinning and depinning of crack fronts in heterogeneous materials*, Phys. Rev. Lett., **78**, (1997) 1062.
- [13] A. Delaplace, J. Schmittbuhl, K.J. Måløy, *High resolution description of a crack front in a heterogeneous Plexiglas block*, Phys. Rev. **E60** (1999) 1337
- [14] D.S. Fisher, *On planar crack wave damping from viscoelasticity*, unpublished.

- [15] A. Pinault, D. Francois, A. Zaoui, *Comportement mécanique des matériaux*, Hermes, Paris (1995)
- [16] H. Gao, J. R. Rice, *A first-order perturbation analysis of crack trapping by arrays of obstacles*, J. Appl. Mech. **56** (1989) 828
- [17] C. Guthmann, R. Gombrowicz, V. Repain, E. Rolley, Phys. Rev. Lett, *Roughness of the Contact Line on a Disordered Substrate* **80** (1998) 2865
- [18] A. Hansen, E. L. Hinrichsen, S. Roux, Phys. Rev. Lett, *Roughness of crack interfaces* **66** (1991) 2476
- [19] A. Hazareesing, M. Mézard, *Wandering of a contact line at thermal equilibrium*, Phys. Rev. **E 60** (1999) 1269
- [20] J. Hodgdon, J.P. Sethna, *Derivation of a general three-dimensional crack-propagation law: A generalization of the principle of local symmetry*, Phys. Rev. **B 47** (1993) 4831.
- [21] D. Hull, P. Beardmore, *Velocity of propagation of cleavage cracks in tungsten*, Int. J. Frac. **2** (1966) 468
- [22] A. Rosso, W. Krauth, *Roughness at the depinning threshold for a long-range elastic string*, e-print cond-mat/0107527
- [23] H. Larralde, R. Ball, *The shape of slowly growing cracks*, Europhys. Lett. **30** (1985) 287
- [24] K.J. Måløy, A. Hansen, E. L. Hinrichsen, S. Roux, *Experimental measurements of the roughness of brittle cracks*, Phys. Rev. Lett., **68**, 213, 1992.
- [25] K. Måløy and J. Schmittbuhl, *Dynamical events during slow crack propagation*, Phys. Rev. Lett., in press, 2001
- [26] B.B. Mandelbrot, D.E. Passoja, A.J. Paullay, *Fractal character of fracture surfaces of metals*, Nature (London), **308**, 721, 1984
- [27] J. W. Morrissey, J. R. Rice, *Crack front waves*, J. Mech. Phys. Solids **46** (1998) 467
- [28] J. W. Morrissey, J. R. Rice, *Perturbative simulations of crack front waves*, J. Mech. Phys. Solids **48** (2000) 122
- [29] A. Parisi, G. Caldarelli, L. Pietronero, *Roughness of fracture surfaces*, e-print cond-mat/0004374
- [30] F. Paun, E. Bouchaud, *Morphology of damage cavities*, in preparation.

- [31] G. Perrin, J. R. Rice, *Disordering of a dynamic planar crack front in a model elastic medium of randomly variable toughness*, J. Mech. Phys. Solids **42** (1994) 1047
- [32] S. Ramanathan, D.S. Fisher, *Dynamics and instabilities of planar tensile cracks in heterogeneous media*, Phys. Rev. Lett. **79** (1997) 877
- [33] S. Ramanathan, D. Ertas, and D. S. Fisher, *Quasi-static crack propagation in heterogeneous media*, Phys. Rev. Lett. **79** (1997) 873
- [34] S. Ramanathan and D. S. Fisher, *Onset of Propagation of Planar Cracks in Heterogeneous Media*, Phys. Rev **B 58**, 6026 (1998)
- [35] S. Ramanathan and D.S. Fisher, *Corrugation waves in dynamic fracture*, in preparation
- [36] K. Ravi-Chandar and B. Yang, *On the role of microcracks in the dynamic fracture of brittle materials*, Journal of Mechanics and Physics of Solids, **45**, (1997), 535-563.
- [37] J. R. Rice, *First order variation in elastic fields due to variation in location of a planar crack front*, J. Appl. Mech. **52** (1985) 571
- [38] J. Schmittbuhl, S. Roux, J.P. Vilotte, K. J. Måløy, *Interfacial crack pinning: effect of non local interactions*, Phys. Rev. Lett. **74** (1995) 1787.
- [39] J. Schmittbuhl, K.J. Måløy, *Direct observation of a self-affine crack propagation*, Phys. Rev. Lett. **78** (1997) 3888
- [40] J. Schmittbuhl, J.P. Vilotte, *Interfacial crack front wandering: influence of quenched noise correlations*, Physica **A270** (1999) 42
- [41] J. Schwarz and D.S. Fisher *Effects of stress pulses on depinning transitions in elastic media*, in preparation
- [42] E. Sharon, G. Cohen, J. Fineberg, *Propagating solitary waves along a rapidly moving crack front*, Nature, **410** (2001) 68
- [43] L. Van Brutzel, *Contribution á l'étude des mécanismes de rupture dans les amorphes*, Ph. D. Dissertation, Paris VI, 1999, unpublished.
- [44] H. Wallner, *Linienstrukturen an bruchflächen*, Z. Physik, **114** (1939) 368
- [45] J. R. Willis, A. B. Movchan, *Dynamic weight functions for a moving crack. I. Mode I loading*, J. Mech. Phys. Solids, **43** (1995) 319
- [46] J. R. Willis, A. B. Movchan, *Three-dimensional dynamic perturbation of a propagating crack*, J. Mech. Phys. Solids, **45** (1997) 591